Journal of Power Sources 218 (2012) 93–99

Contents lists available at SciVerse ScienceDirect

Journal of Power Sources

journal homepage: www.elsevier.com/locate/jpowsour

# Promotion effect of $TiO_2$ on catalytic activity and stability of Pt catalyst for electrooxidation of methanol

Qing Lv [a,b], Min Yin [a,b], Xiao Zhao [a,b], Chenyang Li [a,c], Changpeng Liu [a,**], Wei Xing [a,c,*]

[a] State Key Laboratory of Electroanalytical Chemistry, Changchun Institute of Applied Chemistry, Chinese Academy of Sciences, Changchun, Jilin 130022, China
[b] Graduate School of the Chinese Academy of Sciences, Beijing 100039, China
[c] Laboratory of Advanced Power Sources, Changchun Institute of Applied Chemistry, 5625 Renmin Street, Changchun 130022, PR China

## HIGHLIGHTS

- C and $TiO_2$ are mixed up physically as the hybrid support of Pt.
- Methanol oxidation activity and stability on Pt/$TiO_2$–C catalyst were improved.
- Pt and $TiO_2$ interaction facilitates CO removal and hinders CO formation during methanol oxidation.
- The promotion effect should be attributed to the presence of $TiO_2$.

## ARTICLE INFO

*Article history:*
Received 15 March 2012
Received in revised form
11 June 2012
Accepted 12 June 2012
Available online 20 June 2012

*Keywords:*
Titanium dioxide
Electrocatalysts
Metal-support interaction
Methanol electrooxidation
Fuel cells

## ABSTRACT

$TiO_2$ and C are mixed up physically as hybrid support of Pt nanoparticles for methanol electrooxidation. The morphology and electrocatalytic properties of the as-obtained catalysts have been investigated by transmission electron microscope, X-ray diffraction, X-ray photoelectron spectroscopy, cyclic voltammetry and chronoamperometry. The catalytic activity and stability of Pt/$TiO_2$–C catalyst are both improved markedly compared with that of Pt/C catalyst. The initial and final current of Pt/$TiO_2$–C catalyst after 3600 s reactions for methanol oxidation is about 1.57 and 6 times as high as that of the Pt/C catalyst, respectively. The promotion effect of $TiO_2$ on catalytic activity and stability for Pt/$TiO_2$–C catalyst is investigated further by physical and electrochemical measurements. It is found that the addition of $TiO_2$ could facilitate CO removal, hinder CO formation on Pt surface during methanol oxidation, and inhibit the agglomeration and corrosion of Pt particles, which can be resulted from the strong interaction between $TiO_2$–C and Pt.



## 1. Introduction

The electrooxidation of methanol has attracted much attention because direct methanol fuel cells (DMFCs) are considered as prospective power sources for portable electronic devices due to their suitable power range for small electronic devices, high energy efficiency, and ambient operating conditions [1–5]. At present, carbon supported Pt-based catalysts are commonly used as anode catalysts in DMFCs [6–8]. However, the low catalytic activity and stability of these catalysts in methanol electrooxidation are still one of the important hinders for the commercialization of DMFCs because of the low intrinsic activity of metal nanoparticles, the weak interactions between Pt and carbon support, the dissolution of Pt elements and electrochemical corrosion of the carbon support [9].

To overcome these problems, one approach is to introduce the novel support materials (such as $SnO_2$ [10,11], $WO_3$ [12,13], $CeO_2$ [14–16]) with co-catalytic functionality as the substitute of carbon to improve both the catalytic activity and the durability of Pt-based catalysts. To date, the unique physical and chemical properties of $TiO_2$ [17,18] have made it attract increasing attention as alternative catalyst supports due to excellent mechanical resistance and stability in acidic and oxidative environments. There have been many reports using $TiO_2$ as support of Pt or PtRu for methanol oxidation [19,20]. The effect of $TiO_2$ on Pt/$TiO_2$ catalyst has been studied by Yoo et al. [21]. However, $TiO_2$ has some own defects such as the low electric conductivity and surface area. It seems more reasonable to combine carbon and $TiO_2$ to make hybrid support for

* Corresponding author. State Key Laboratory of Electroanalytical Chemistry, Changchun Institute of Applied Chemistry, Chinese Academy of Sciences, Changchun, Jilin, 130022, China. Tel.: +86 431 85262223; fax: +86 431 85685653.
** Corresponding author. Tel: +86 431 85262225.
*E-mail addresses:* liuchp@ciac.jl.cn (C. Liu), xingwei@ciac.jl.cn (W. Xing).

0378-7753/$ – see front matter © 2012 Elsevier B.V. All rights reserved.
http://dx.doi.org/10.1016/j.jpowsour.2012.06.051

Pt-based catalysts. For example, Zheng et al. [22] has pointed that the Pt/$TiO_2$–C could possess enhanced stability in aqueous solution of sulfuric acid in comparison with Pt/C. It becomes very necessary to study the effect of $TiO_2$ on Pt/$TiO_2$–C catalyst for methanol oxidation.

In order to investigate the real effect of $TiO_2$ on Pt/C catalyst for methanol oxidation, in the present study, $TiO_2$ and Vulcan XC-72 carbon black were physical mixed as the hybrid support to support the Pt catalysts. This Pt/$TiO_2$–C catalyst was characterized by X-ray diffraction, transmission electron microscope, X-ray photoelectron spectroscopy and electrochemical measurements compared with the Pt/C catalyst prepared in the same way. It was found that Pt/$TiO_2$–C catalyst exhibited both excellent catalytic activity and stability for methanol electrooxidation. Moreover, the single fuel cell results confirmed that the performance of Pt/$TiO_2$–C was really improved as anodic catalyst.

## 2. Experimental

### 2.1. Catalyst preparation

Pt/$TiO_2$–C catalyst (20 wt% Pt, 20 wt% $TiO_2$) was prepared by microwave-assisted polyol reduction method. Firstly, 60 mg Vulcan XC-72 carbon black and 20 mg $TiO_2$ were ultrasonically suspended in ethylene glycol for 2 h and then aqueous solution of $H_2PtCl_6$ was added into the suspension. After the mixture was stirred vigorously for 4 h, the pH was adjusted to 12 by ethylene glycol solution containing NaOH with stirring. Then, the mixture was placed in the center of a microwave oven (2450 MHz, 750 W) and heated for 50 s, following by stirring for another 8 h. The reaction solutions were filtered with filter paper and washed with ethanol and triply distilled water until no $Cl^-$ was detected. At last, the obtained catalyst was dried in a vacuum oven at 80 °C overnight. The preparation method of Pt/C catalysts was similar to that mentioned above except that $TiO_2$ was not added.

### 2.2. Materials characterizations

The X-ray diffraction (XRD) patterns of the catalysts were obtained using a Rigaku-D/MAX-PC2500 X-ray diffractometer (Japan) with the Cu Kα ($\lambda = 1.5405$ Å) as a radiation source operating at 40 kV and 200 mA. Transmission electron microscope (TEM) analysis was carried out with a JEOL2010 microscope operating at 200 kV with nominal resolution. Samples were firstly ultrasonicated in alcohol for 1 h and then deposited on 3 mm Cu grids. X-ray photoelectron spectroscopy (XPS) was recorded on a Kratos XSAM-800 spectrometer with an Al Kα monochromatic source. The C 1 s peak was used as a reference.

Electrochemical measurements were carried out with a Princeton Applied Research Model273 Potentiostat/Galvanostat and a conventional three electrode electrochemical cell. A Pt plate was used as the counter electrode. The saturated calomel electrode (SCE) was used as the reference electrode which was connected to the working electrode by a Luggin capillary. All of the potentials in this study were reported with respect to SCE unless otherwise mentioned. The glassy carbon electrode was polished with slurry of 0.3 μm and 0.05 μm alumina successively and washed ultrasonically in deionized water prior to use. All the electrochemical measurements were carried out at 25 ± 1 °C. The catalyst ink was prepared by ultrasonically dispersing the mixture of 5 mg catalysts, 1510 μL ethanol, and 90 μL 5wt.% Nafion solutions. 8 μL catalyst inks was pipetted and spread on the glassy carbon disk with 5 mm diameter (the Pt loading on the electrode is 25.5 μg $cm^{-2}$). Finally, the electrode was obtained after the solvent volatilized. $N_2$ was purged for 20 min before starting the electrochemical experiments at flow rate of ca. 100 mL $min^{-1}$, unless otherwise mentioned. The CO stripping voltammograms were measured in the 0.5 M $H_2SO_4$ solution. CO was purged into the 0.5 M $H_2SO_4$ solution adsorption for 15 min to allow the complete adsorption of CO onto the catalyst when the working electrode was kept at 0.1 V, and then excess CO in the electrolyte was removed by purging $N_2$ for 30 min at flow rate of ca. 100 mL $min^{-1}$unless otherwise mentioned.

### 2.3. Single cell test

The performance of a single DMFC with the anodic Pt/$TiO_2$–C (20 wt% Pt) catalyst was measured and compared with that with the anodic Pt/C catalyst (20 wt% Pt). Pt/C catalyst (20 wt.% Pt) was used as the cathodic catalyst. The membrane electrode assembly (MEA) was fabricated according to the procedure reported in the literature [23]. The geometrical area of the anode and cathode electrode was 3 cm × 3 cm (9 $cm^2$). The catalyst loading in both the anode and cathode was 4 mg $cm^{-2}$. The performance of the single cell was measured with a Fuel Cell Test System (Arbin Co.). 2.0 M $CH_3OH$ solution with a flow rate of 10 mL $min^{-1}$ and oxygen with a flow rate of 200 mL $min^{-1}$ at 1 atm were used. The single cell was operated at 25 °C. The stability test was carried out at 0.1 A right after the polarization test.

## 3. Results and discussion

Fig. 1 shows the XRD patterns of the Pt/C catalyst, Pt/$TiO_2$–C catalyst and the $TiO_2$–C support. The characteristic $TiO_2$ diffraction peaks were clearly observed in Pt/$TiO_2$–C catalyst. For all samples, the peak at ca. 25° could be attributed to the (002) plane reflection of carbon. For all Pt in as-prepared catalysts, the characteristic peaks at ca. 40, 46, 68 and 82° corresponded to (111), (200), (220) and (311) plane of face centered cubic Pt, respectively. No shift was observed at the positions of the Pt diffraction peaks in the Pt/$TiO_2$–C catalyst, compared with that in the Pt/C catalyst, indicating that the addition of $TiO_2$ had no effect on the crystalline lattice of Pt.

The TEM images of the Pt/$TiO_2$–C and Pt/C catalysts are shown in Fig. 2A and B, respectively. For both catalysts, it could be found that the Pt nanoparticles were uniformly dispersed on the support. The average particle size of Pt in Pt/C and Pt/$TiO_2$–C catalyst was ca. 2.67 and 2.96 nm, respectively. These results indicated that the addition of $TiO_2$ had no obvious effect on the location of Pt

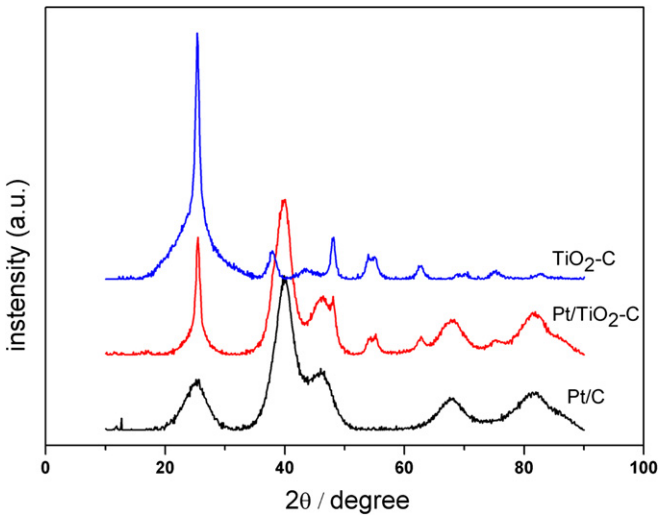


**Fig. 1.** XRD patterns of Pt/C catalyst, Pt/$TiO_2$–C catalyst and the $TiO_2$–C support.

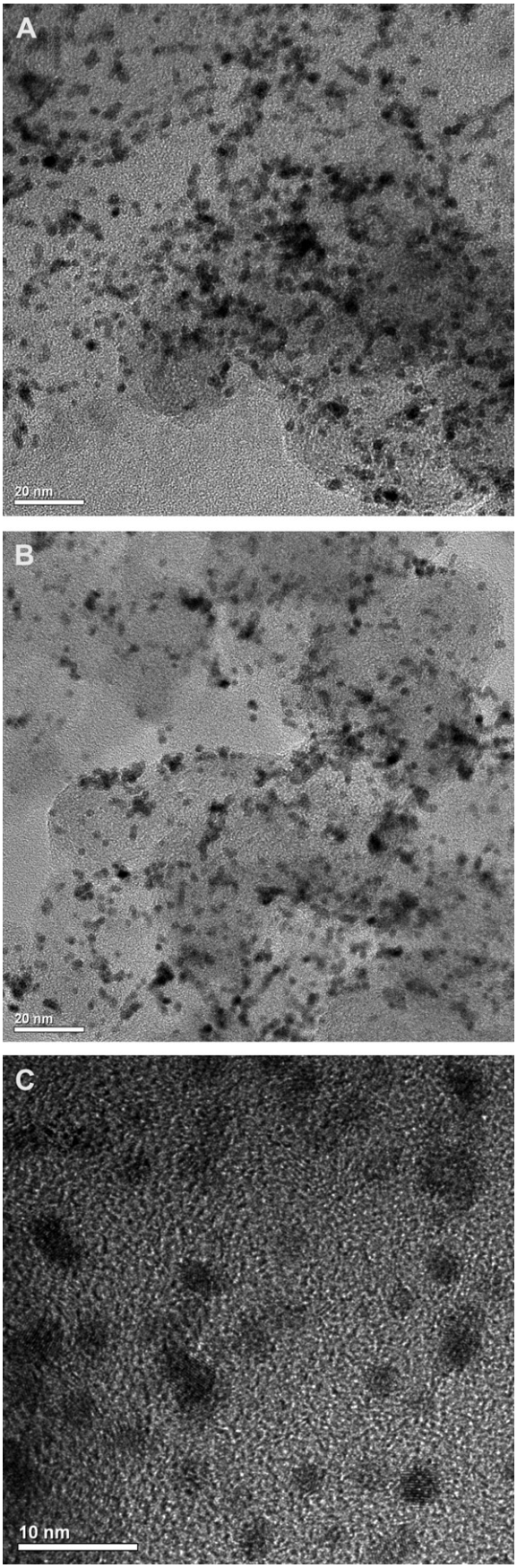


**Fig. 2.** TEM image of $Pt/TiO_2$–C (A) and Pt/C (B) catalysts; HRTEM image of $Pt/TiO_2$–C (C) catalyst.

nanoparticles on supports. Besides, according to the HRTEM image of $Pt/TiO_2$–C catalyst (Fig. 2C), Pt was mostly deposited on carbon.

The XPS Pt 4f spectra of $Pt/TiO_2$–C and Pt/C catalysts are shown in Fig. 3. The binding energies of all peaks were referenced to a C 1s value of 284.6 eV. For the Pt/C catalyst, the spectrum of Pt (4f) shows a doublet containing a low binding energy ($4f_{7/2}$) at 70.7 eV and a high binding energy ($4f_{5/2}$) at 74.2 eV. For the $Pt/TiO_2$–C catalyst, the low binding energy peak was located at 70.4 eV, which was negatively shifted by 0.3 eV, and the high binding energy peak (at 73.8 eV) was also negatively shifted by 0.4 eV compared to the Pt/C catalyst. The shift of the Pt 4f position for the Pt catalysts indicated that the electronic properties of Pt were changed by incorporating $TiO_2$ as the support, which could weaken the bonding energy between metal and strongly adsorbed poisoning species [24–26]and result in the variable catalytic properties according to the so-called electronic effect [27–29]. The negative shift of the binding energy of Pt (4f) in $Pt/TiO_2$–C catalyst could be resulted from the stronger interaction between the Pt and $TiO_2$–C support, compared with the Pt/C catalyst. As shown in Fig. 3, the Pt 4f signal of $Pt/TiO_2$–C and Pt/C was deconvolved into two pairs of doublets, which were attributed to metallic Pt(0) and Pt(II) in PtO or $Pt(OH)_2$ like species. The content of Pt (0) increases by 25% because the addition of $TiO_2$ demonstrating that $Pt/TiO_2$–C catalyst has higher stability due to greater corrosion resistance of Pt (0) [30].

Fig. 4 shows the cyclic voltammograms (CVs) of the catalysts in 0.5 M $H_2SO_4$. The electrochemical surface area (ESA) of the catalyst could be calculated [16,31–33] by assuming charge density of 210 $\mu C\ cm^{-2}$ of hydrogen adsorption on polycrystalline Pt electrode. The ESA of the Pt/C and $Pt/TiO_2$–C catalysts was 62.0 and 60.0 $m^2\ g^{-1}$, respectively. The similar ESA of the two catalysts could be related to the similar dispersion condition and nanoparticle size for both catalysts from the TEM image. In addition, both Pt oxidation onset potential and Pt–O reduction peak potential for $Pt/TiO_2$–C catalyst had a positive shift compared to that for Pt/C catalyst, indicating that the $Pt/TiO_2$–C catalyst possesses reduced oxophilicity and a weakened chemical adsorption energy with oxygen-containing species, such as $CO_{ad}$ and $OH_{ad}$ on Pt surface [34], which agreed well with the XPS results.

The area-normalized currents for methanol electrooxidation are shown in Fig. 5. The area-normalized current means current was normalized with electrochemical active area. It represents the intrinsic activity of the active sites in the catalysts [35]. It was shown that the $Pt/TiO_2$–C catalyst exhibited higher activity than the Pt/C catalyst. The peak current density for $Pt/TiO_2$–C catalyst was about 1.57 times that of the Pt/C catalyst, which demonstrated the promotion effect of the $TiO_2$ on the electrooxidation of methanol.

In order to test the CO poisoning effect, the $CO_{ad}$ stripping curves of the Pt/C and $Pt/TiO_2$–C catalysts are presented in Fig. 6. The peak potential for $CO_{ad}$ oxidation at the $Pt/TiO_2$–C catalyst was 0.55 V, while that at Pt/C catalyst was 0.58 V. The negative shift of the potential for the $Pt/TiO_2$–C catalyst indicates that $Pt/TiO_2$–C catalyst was more active for the electrooxidation of CO compared to Pt/C catalyst. This could be attributed to the beneficial electronic effect of $TiO_2$–C on Pt, which weakened the bonding energy between Pt and $CO_{ads}$. Then, to compare the different bonding energy between Pt and $CO_{ads}$ in the two catalysts, $N_2$ with high flow rate was used. The flow rate of $N_2$ was doubled to the common $CO_{ad}$ stripping voltammetric experiments after CO was purged into the 0.5 M $H_2SO_4$ solution for 15 min at a fixed potential of 0.1 V in the same condition. The $CO_{ad}$ stripping curves with the flow rate of ca. 200 mL $min^{-1}$ were shown in Fig. 7, while the common $CO_{ad}$ stripping curves with the common flow rate was ca. 100 mL $min^{-1}$ as shown in Fig. 6. The $N_2$ flow time in Fig. 7(A) and (B) was 30 min

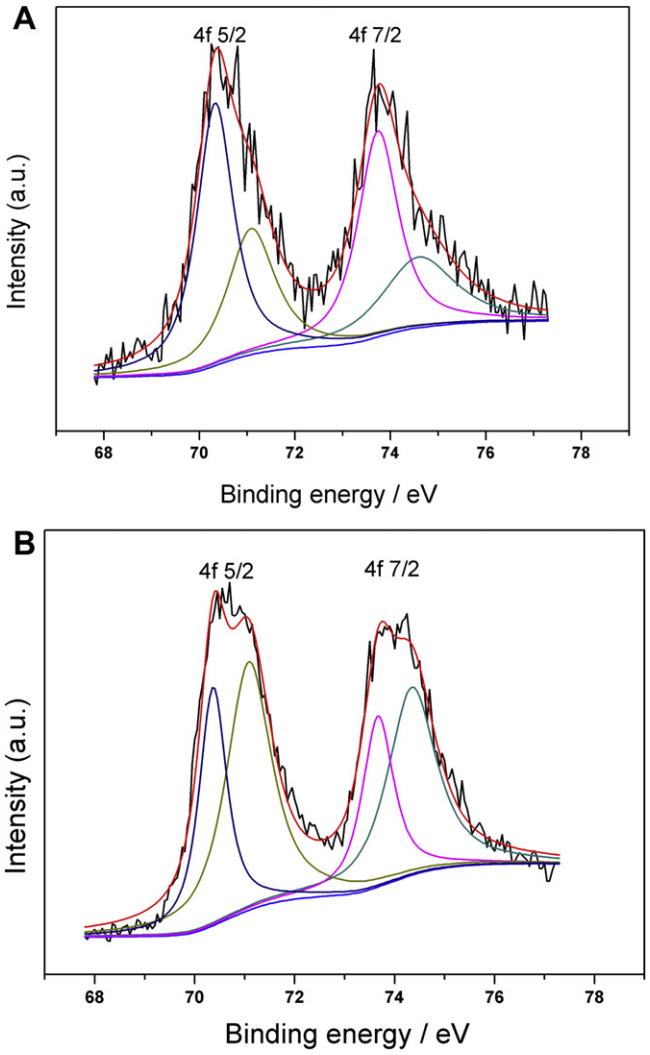


**Fig. 3.** Pt 4f region in the XPS spectra of Pt/$TiO_2$–C (A) and Pt/C (B) catalysts.

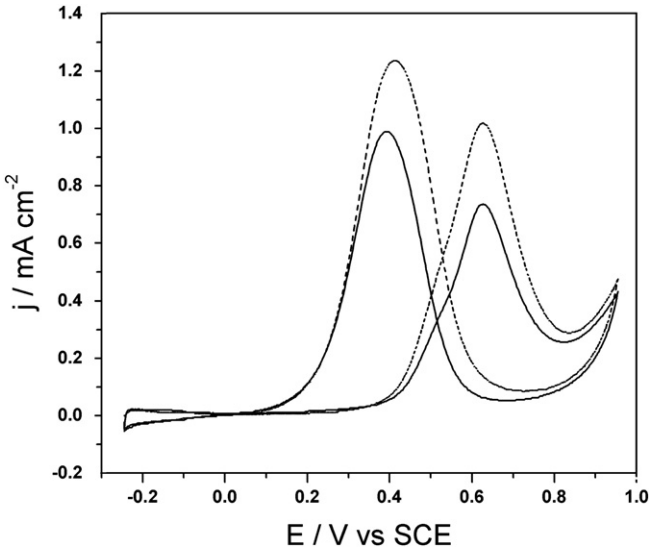


**Fig. 5.** CVs at Pt/C (solid line) and Pt/$TiO_2$–C (dash line) catalysts in 0.5 M $H_2SO_4$ + 1.0 M $CH_3OH$ solution with a scan rate of 50 mV $s^{-1}$.

and 60 min for Pt/C and Pt/$TiO_2$–C catalysts, respectively. For the Pt/C catalyst, the peak current of CO oxidation in Fig. 7 was ca. 0.59 mA and 0.53 mA at the $N_2$ flow time of 30 min and 60 min, respectively. For Pt/$TiO_2$–C catalyst, the peak current of CO oxidation in Fig. 7 was ca. 0.46 mA and 0.23 mA at the $N_2$ flow time of 30 min and 60 min, respectively. The decrease of the peak current of CO oxidation indicated that the purging $N_2$ at high flow rate could destroy the combination between Pt and CO. The larger change of the peak current of CO oxidation at Pt/$TiO_2$–C catalyst than at Pt/C catalyst means that the adsorbed CO at Pt/$TiO_2$–C catalyst was easier to be affected than Pt/C catalyst, which was consistent with the result of XPS. This weak bonding energy facilitated the CO removal on Pt surface for Pt/$TiO_2$–C catalyst.

To further demonstrate the CO formation during methanol oxidation on the catalysts, chronoamperometric (CA) measurements at 0.3 V in methanol solutions were carried out to collect $CO_{ads}$ on Pt surface during methanol oxidation reactions. Then, CVs were conducted on these CO adsorbed Pt electrode to determine

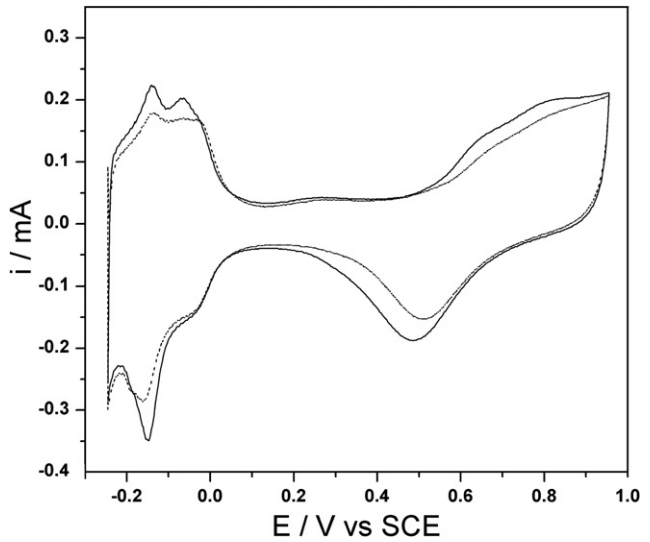


**Fig. 4.** CVs at Pt/$TiO_2$–C (solid line) and Pt/C (dash line) catalysts in 0.5M $H_2SO_4$ solution with a scan rate of 50 mV $s^{-1}$.

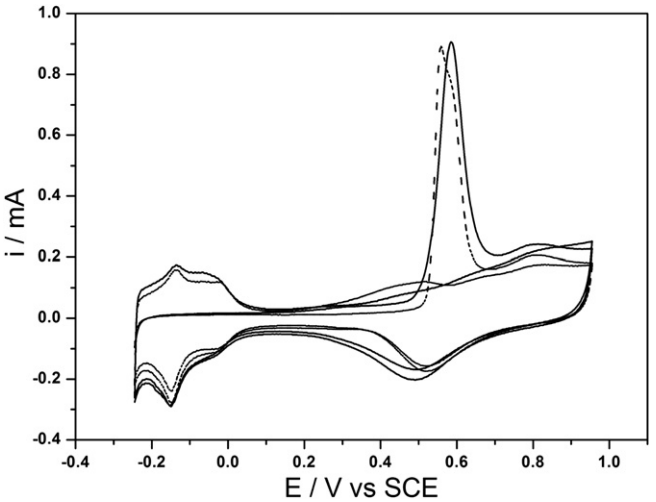


**Fig. 6.** The $CO_{ad}$ stripping voltammogram for Pt/C (solid line) and Pt/$TiO_2$–C (dash line) catalysts in 0.5M $H_2SO_4$ solution with a scan rate of 50 mV $s^{-1}$. The flow rate of $N_2$ was ca. 100 mL $min^{-1}$.

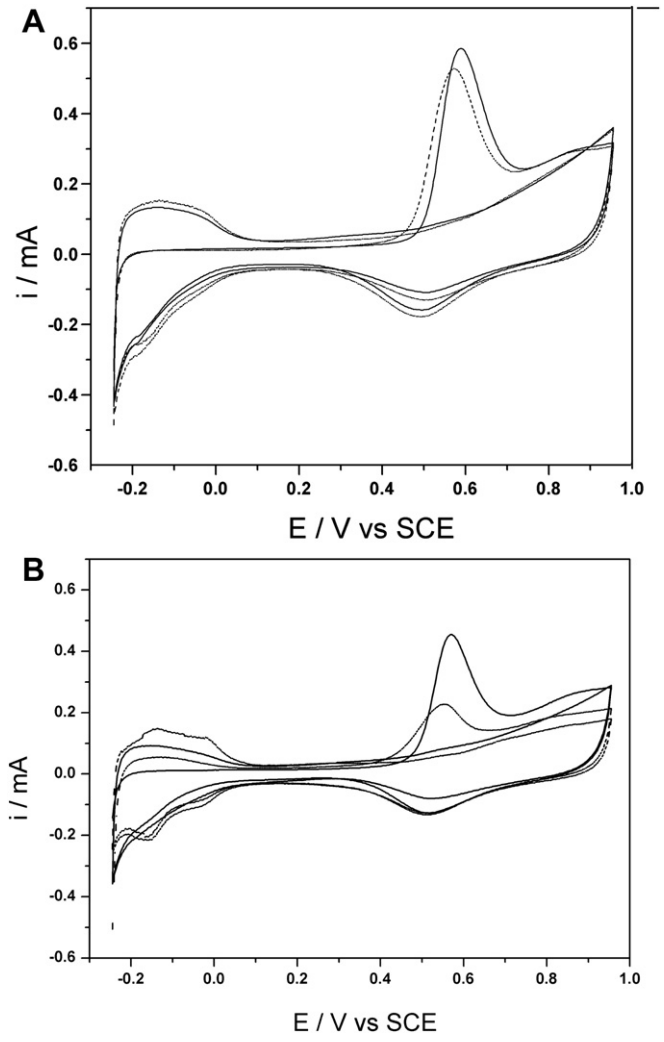


**Fig. 7.** The "$CO_{ad}$ stripping voltammogram" for Pt/C (A) and Pt/$TiO_2$–C (B) catalysts in 0.5M $H_2SO_4$ solution with a scan rate of 50 mV $s^{-1}$. CO adsorption at the catalysts was done at a fixed potential of 0.1 V in 0.5 M $H_2SO_4$ solution with CO flow for 15 min, and then $N_2$ was flowed for 30 min (solid line) and 60 min (dash line) at a rate of ca. 200 mL $min^{-1}$ which was twice as common flow rate.

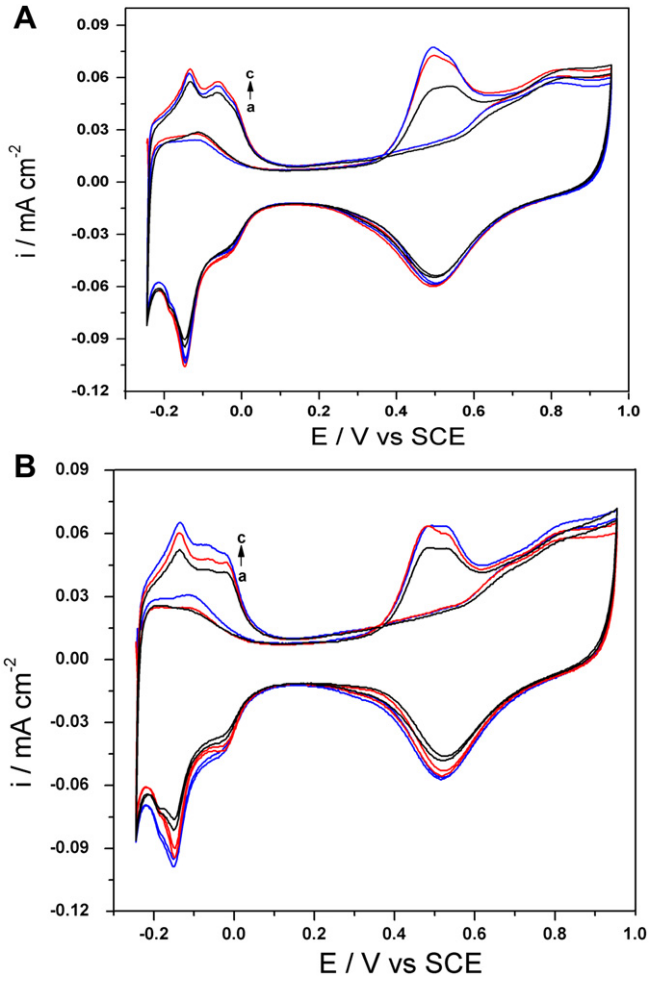


**Fig. 8.** The first two cycles of CVs for Pt/C (A) and Pt/$TiO_2$–C (B) catalysts in 0.5 M $H_2SO_4$ after the potential fixed at 0.3 V for 200 s (black), 400 s (red) and 600 s (blue), respectively, in 1.0 M $CH_3OH$ + 0.5 M $H_2SO_4$ solution. (For interpretation of the references to color in this figure legend, the reader is referred to the web version of this article.)

the adsorbed CO quantity. CVs after different time of CA measurements for 200 s, 400 s or 600 s in 1.0 M $CH_3OH$ and 0.5 M $H_2SO_4$ solution were shown in Fig. 8. According to the previous study [36,37], it was known that the peak between ca. 0.35 V and 0.65 V was $CO_{ad}$ oxidation peak from methanol oxidation. In our experiment, the onset potential of CO oxidation was about 0.35 V. Thus, the potential was fixed at 0.3 V to avoid the oxidation of CO formed on Pt surface. To determine the $CO_{ad}$ surface concentration, the current was normalized by the electrochemical surface area of the active sites. It was obvious that the peak area of CO oxidation was increased with the time of constant-potential measurement prolonged from 200 s to 400 s, However, when the time was prolonged further, the peak area of CO oxidation remained almost the same. It showed the adsorbed CO on the electrode was already saturated. The peak area of CO oxidation for the Pt/$TiO_2$–C catalyst was ca. three quarters of that for the Pt/C catalyst. It suggested that the CO formation on Pt/$TiO_2$–C catalyst during methanol oxidation was also smaller than that on Pt/C catalyst.

In order to investigate the stability of the catalysts, Fig. 9 presents the CA curves of Pt/C and Pt/$TiO_2$–C catalysts at the fixed potential of 0.45 V for 3600 s in a 0.5 M $H_2SO_4$ solution containing 1.0 M $CH_3OH$. The final current density of the Pt/$TiO_2$–C catalyst was 0.178 mA $cm^{-2}$, which was about 6 times as high as that of Pt/C catalyst (0.030 mA $cm^{-2}$). It means that the Pt/$TiO_2$–C catalyst could possess 36.6% of the initial current value after 3600 s reaction, while the Pt/C catalyst had only 7.0% of its own initial value. These results concluded that the Pt/$TiO_2$–C catalyst could be an excellent catalyst for methanol oxidation due to both superior catalytic activity and stability.

The decreased ESA of the catalysts due to the corrosion of the metal and support was an important factor to affect the stability of catalysts in DMFCs [20,38]. Thus, to determine the changes of the ESA for Pt/C and Pt/$TiO_2$–C catalysts, CVs were conducted after different reaction times such as 0 h, 1 h, 3 h and 5 h during CA measurements, as shown in Fig. 10. It was obvious that the ESA change of Pt/C catalyst was much larger than that of Pt/$TiO_2$–C catalyst. The ESA of Pt/C catalyst decreased by ca. 13%, 28% and 30%, respectively, after the CA measurements of 1 h, 3 h and 5 h, while the ESA of Pt/$TiO_2$–C catalyst decreased only by ca. 3%, 4% and 8%, respectively, after 1 h, 3 h and 5 h CA measurements. The less change of the ESA for Pt/$TiO_2$–C catalyst could be one of the reasons for the superior stability of the catalyst. It could be resulted from the strong interaction between Pt and the $TiO_2$–C support, which could suppress the agglomeration of Pt particles and the corrosion

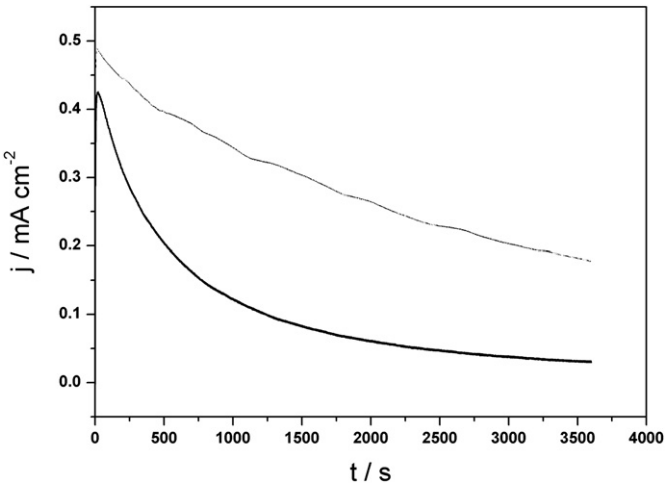


**Fig. 9.** Chronoamperometric curves at Pt/C (solid line) and Pt/$TiO_2$–C (dash line) catalysts in 0.5 M $H_2SO_4$ + 1.0 M $CH_3OH$ solution with a scan rate of 50 mV $s^{-1}$.

of Pt and the hybrid support. The hindered Pt corrosion for Pt/$TiO_2$–C catalyst was also consistent well with the XPS result.

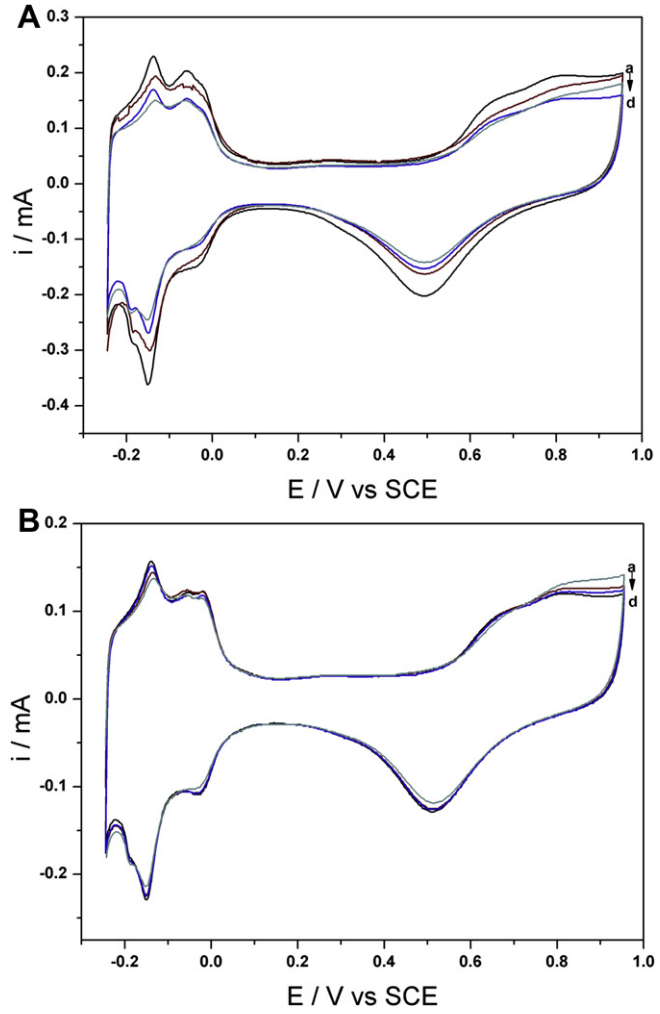


**Fig. 10.** CVs at Pt/C (A) and Pt/$TiO_2$–C (B) catalysts after the chronoamperometric measurements of 0 h (a), 1 h (b), 3 h (c) and 5 h (d) at fixed potential of 0.45 V in 0.5 M $H_2SO_4$ + 1.0 M $CH_3OH$ solution with a scan rate of 50 mV $s^{-1}$.

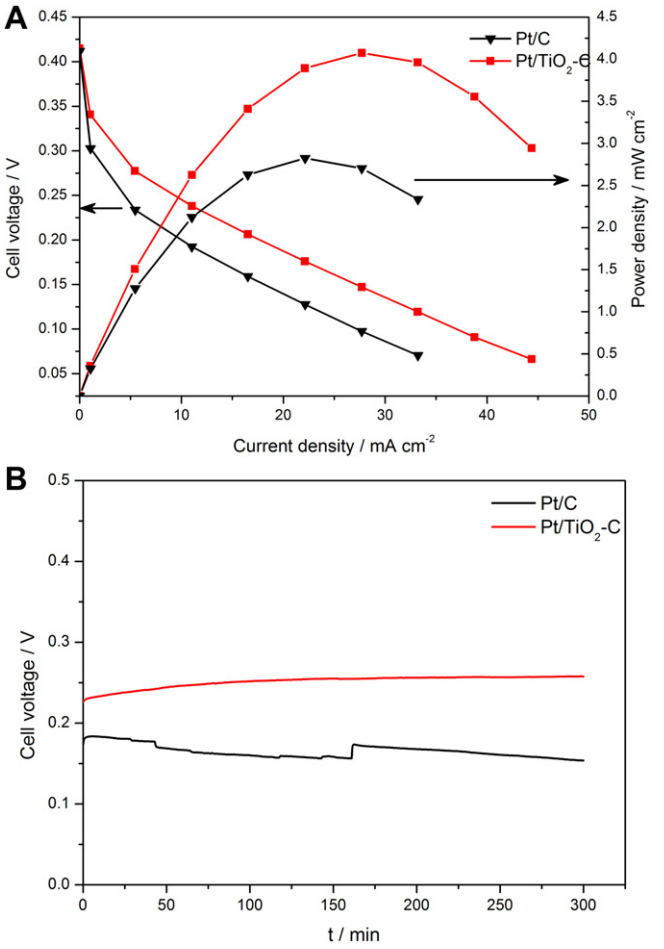


**Fig. 11.** (A) Polarization and power density curves of DMFCs with Pt/C and Pt/$TiO_2$–C anodic catalysts; (B) stability test at 0.1A of DMFCs with Pt/C and Pt/$TiO_2$–C anodic catalysts.

Fig. 11(A) compares the polarization and power density curves of the single DMFC with different anodic catalysts. The Pt/$TiO_2$–C performed much better than Pt/C as the anodic catalyst. The single cell with Pt/$TiO_2$–C has approximately 46% higher maximum power density (4.1 mW $cm^{-2}$) than that of Pt/C (2.8 mW $cm^{-2}$). This result is consistent with that of CVs. The stability test of the single DMFC is shown in Fig. 11(B). The voltage of DMFC with Pt/C has a slight decrease, while the voltage of DMFC with Pt/$TiO_2$–C has a slight increase during the 300 min test. This result is also consistent with that of CA.

## 4. Conclusion

The physical mixture of C and $TiO_2$ was successfully used as a support for Pt catalyst on methanol electrooxidation. $TiO_2$ addition has little effect on the particle size and distribution of obtained Pt nanoparticles on support. The catalytic activity and the stability on Pt/$TiO_2$–C catalyst for methanol oxidation were both improved greatly compared with that on Pt/C catalyst. Electrochemical results showed that the CO removal on Pt surface could be facilitated on Pt/$TiO_2$–C catalyst due to the lower bonding energy between Pt and $CO_{ads}$ on Pt/$TiO_2$–C catalyst than that on Pt/C catalyst. Furthermore, the CO formation during methanol oxidation was also found to be decreased greatly on Pt/$TiO_2$–C catalyst in comparison with Pt/C catalyst. The stability test showed that the agglomeration of Pt particles as well as the corrosion of Pt and the support during

methanol oxidation could be suppressed greatly by the addition of $TiO_2$. These results confirmed that this simply prepared $Pt/TiO_2$–C material could be a promising catalyst for the anode in direct methanol fuel cell.

## Acknowledgement

This work was supported by the High Technology Research Program (863 program, 2012AA053401) of the Science and Technology Ministry of China, National Basic Research Program of China (973 Program, Nos. 2012CB932802 and 2012CB215500), General Programs of National Natural Science Foundation of China (20876153, 21011130027), the Science & Technology Research Programs of Jilin Province (20100420).

## References

[1] Z. Liu, X.Y. Ling, B. Guo, L. Hong, J.Y. Lee, J. Power Sources 167 (2007) 272–280.
[2] C. Alegre, L. Calvillo, R. Moliner, J.A. González-Expósito, O. Guillén-Villafuerte, M.V.M. Huerta, E. Pastor, M.J. Lázaro, J. Power Sources 196 (2011) 4226–4235.
[3] Z. Jusys, R.J. Behm, J. Phys. Chem. B 105 (2001) 10874–10883.
[4] X. Zhao, M. Yin, L. Ma, L. Liang, C. Liu, J. Liao, T. Lu, W. Xing, Energy Environ. Sci. (2011).
[5] L. Feng, Q. Lv, X. Sun, S. Yao, C. Liu, W. Xing, J. Electroanal. Chem. 664 (2012) 14–19.
[6] Y. Shimazaki, S. Hayasaka, T. Koyama, D. Nagao, Y. Kobayashi, M. Konno, J. Colloid Interface Sci. 351 (2010) 580–583.
[7] Z. Zhou, S. Wang, W. Zhou, G. Wang, L. Jiang, W. Li, S. Song, J. Liu, G. Sun, Q. Xin, Chem. Commun. (2003) 394–395.
[8] R. Borup, J. Meyers, B. Pivovar, Y.S. Kim, R. Mukundan, N. Garland, D. Myers, M. Wilson, F. Garzon, D. Wood, P. Zelenay, K. More, K. Stroh, T. Zawodzinski, J. Boncella, J.E. McGrath, M. Inaba, K. Miyatake, M. Hori, K. Ota, Z. Ogumi, S. Miyata, A. Nishikata, Z. Siroma, Y. Uchimoto, K. Yasuda, K.I. Kimijima, N. Iwashita, Chem. Rev. 107 (2007) 3904–3951.
[9] H. Liu, C. Song, L. Zhang, J. Zhang, H. Wang, D.P. Wilkinson, J. Power Sources 155 (2006) 95–110.
[10] X.W. Lou, D. Deng, J.Y. Lee, L.A. Archer, Chem. Mater. 20 (2008) 6562–6566.
[11] H.L. Pang, X.H. Zhang, X.X. Zhong, B. Liu, X.G. Wei, Y.F. Kuang, J.H. Chen, J. Colloid Interface Sci. 319 (2008) 193–198.
[12] S. Jayaraman, T.F. Jaramillo, S.-H. Baeck, E.W. McFarland, J. Phys. Chem. B 109 (2005) 22958–22966.
[13] Z. Cui, L. Feng, C. Liu, W. Xing, J. Power Sources 196 (2011) 2621–2626.
[14] C.L. Campos, C. Roldán, M. Aponte, Y. Ishikawa, C.R. Cabrera, J. Electroanal. Chem. 581 (2005) 206–215.
[15] D.-M. Gu, Y.-Y. Chu, Z.-B. Wang, Z.-Z. Jiang, G.-P. Yin, Y. Liu, Appl. Catal. B 102 (2011) 9–18.
[16] A.O. Neto, L.A. Farias, R.R. Dias, M. Brandalise, M. Linardi, E.V. Spinacé, Electrochem. Commun. 10 (2008) 1315–1317.
[17] S. S, A. Gedanken, Small (2007) 5.
[18] R.E. Fuentes, B.L. Garcia, J.W. Weidner, J. Electrochem. Soc. 158 (2011) B461–B466.
[19] K. Drew, G. Girishkumar, K. Vinodgopal, P.V. Kamat, J. Phys. Chem. B 109 (2005) 11851–11857.
[20] S.-Y. Huang, P. Ganesan, S. Park, B.N. Popov, J. Am. Chem. Soc. 131 (2009) 13898–13899.
[21] S. Yoo, K.-S. Lee, Y.-H. Cho, S.-K. Kim, T.-H. Lim, Y.-E. Sung, Electrocatalysis 2 (2011) 297–306.
[22] Z.Z. Jiang, Z.B. Wang, Y.Y. Chu, D.M. Gu, G.P. Yin, Energy Environ. Sci. 4 (2011) 728–735.
[23] A.S. Aricò, A.K. Shukla, K.M. El-Khatib, P. Cretì, V. Antonucci, J. Appl. Electrochem. 29 (1999) 673–678.
[24] R.M. Navarro, M.C. Álvarez-Galván, M.C. Sánchez-Sánchez, F. Rosa, J.L.G. Fierro, Appl. Catal. B 55 (2005) 229–241.
[25] J.L. Haan, K.M. Stafford, R.I. Masel, J. Phys. Chem. C 114 (2010) 11665–11672.
[26] Z.H. Zhang, J.J. Ge, L.A. Ma, J.H. Liao, T.H. Lu, W. Xing, Fuel Cells 9 (2009) 114–120.
[27] M.V. Martínez-Huerta, N. Tsiouvaras, M.A. Peña, J.L.G. Fierro, J.L. Rodríguez, E. Pastor, Electrochim. Acta 55 (2010) 7634–7642.
[28] M. Yin, Y. Huang, Q. Lv, L. Liang, J. Liao, C. Liu, W. Xing, Electrochim. Acta 58 (2011) 6–11.
[29] Z. Wang, G. Chen, D. Xia, L. Zhang, J. Alloys Compd. 450 (2008) 148–151.
[30] W. Li, A.M. Lane, Electrochem. Commun. 11 (2009) 1187–1190.
[31] J. Ge, X. Chen, C. Liu, T. Lu, J. Liao, L. Liang, W. Xing, Electrochim. Acta 55 (2010) 9132–9136.
[32] G. Chen, Y. Li, D. Wang, L. Zheng, G. You, C.-J. Zhong, L. Yang, F. Cai, J. Cai, B.H. Chen, J. Power Sources 196 (2011) 8323–8330.
[33] B. Abida, L. Chirchi, S. Baranton, T.W. Napporn, H. Kochkar, J.-M. Léger, A. Ghorbel, Appl. Catal. B 106 (2011) 609–615.
[34] S. Wang, S.P. Jiang, T.J. White, J. Guo, X. Wang, J. Phys. Chem. C 113 (2009) 18935–18945.
[35] J.-M. Lee, S.-B. Han, J.-Y. Kim, Y.-W. Lee, A.R. Ko, B. Roh, I. Hwang, K.-W. Park, Carbon 48 (2010) 2290–2296.
[36] W.L. Xu, T.H. Lu, C.P. Liu, W. Xing, J. Phys. Chem. B 110 (2006) 4802–4807.
[37] Y.X. Chen, A. Miki, S. Ye, H. Sakai, M. Osawa, J. Am. Chem. Soc. 125 (2003) 3680–3681.
[38] Z.-Z. Jiang, D.-M. Gu, Z.-B. Wang, W.-L. Qu, G.-P. Yin, K.-J. Qian, J. Power Sources 196 (2011) 8207–8215.